GLIA 35:189–203 (2001)

Effect of Elevated K^+, Hypotonic Stress, and Cortical Spreading Depression on Astrocyte Swelling in GFAP-Deficient Mice

MIROSLAVA ANDĚROVÁ,[1–3] ŠÁRKA KUBINOVÁ,[1–3] TOMÁŠ MAZEL,[1–3]
ALEXANDR CHVÁTAL,[1–3] CAMILLA ELIASSON,[4]
MILOS PEKNY,[4] AND EVA SYKOVÁ[1–3]*

[1]*Department of Neuroscience, Institute of Experimental Medicine, Academy of Sciences of the Czech Republic, Prague, Czech Republic*
[2]*Department of Neuroscience, Charles University, Second Medical Faculty, Prague, Czech Republic*
[3]*Center for Cell Therapy and Tissue Repair, Charles University, Prague, Czech Republic*
[4]*Department of Medical Biochemistry, University of Göteborg, Göteborg, Sweden*

KEY WORDS glial fibrillar acidic protein; intermediate filaments; extracellular potassium; patch-clamp; gray matter; TMA^+ iontophoretic method; diffusion parameters; spinal cord; cortex

ABSTRACT Glial fibrillary acidic protein (GFAP) is the main component of intermediate filaments in astrocytes. To assess its function in astrocyte swelling, we compared astrocyte membrane properties and swelling in spinal cord slices of 8- to 10-day-old wild-type control ($GFAP^{+/+}$) and GFAP-knockout ($GFAP^{-/-}$) mice. Membrane currents and K^+ accumulation around astrocytes after a depolarizing pulse were studied using the whole-cell patch-clamp technique. In vivo cell swelling was studied in the cortex during spreading depression (SD) in 3 to 6-month-old animals. Swelling-induced changes of the extracellular space (ECS) diffusion parameters, i.e., volume fraction α and tortuosity λ, were studied by the real-time iontophoretic tetramethylammonium (TMA^+) method using TMA^+-selective microelectrodes. Morphological analysis using confocal microscopy and quantification of xy intensity profiles in a confocal plane revealed a lower density of processes in $GFAP^{-/-}$ astrocytes than in $GFAP^{+/+}$ astrocytes. K^+ accumulation evoked by membrane depolarization was lower in the vicinity of $GFAP^{-/-}$ astrocytes than $GFAP^{+/+}$ astrocytes, suggesting the presence of a larger ECS around $GFAP^{-/-}$ astrocytes. Astrocyte swelling evoked by application of 50 mM K^+ or by hypotonic solution (HS) produced a larger increase in $[K^+]_e$ around $GFAP^{+/+}$ astrocytes than around $GFAP^{-/-}$ astrocytes. No differences in α and λ in the spinal cord or cortex of $GFAP^{+/+}$ and $GFAP^{-/-}$ mice were found; however, the application of either 50 mM K^+ or HS in spinal cord, or SD in cortex, evoked a large decrease in α and an increase in λ in $GFAP^{+/+}$ mice only. Slower swelling in $GFAP^{-/-}$ astrocytes indicates that GFAP and intermediate filaments play an important role in cell swelling during pathological states. *GLIA 35:189–203, 2001.*

INTRODUCTION

Glial fibrillary acidic protein (GFAP) represents the major constituent of intermediate filaments (IFs) and is specifically expressed in astrocytes (Eng et al., 1971, 2000; Bignami et al., 1972; Uyeda et al., 1972; Bignami and Dahl, 1977).

To study the function of GFAP, mutant mice lacking GFAP ($GFAP^{-/-}$) have been introduced (Gomi et al., 1995; Pekny et al., 1995; Liedtke et al., 1996; McCall et

Grant sponsor: the Grant Agency of the Czech Republic; Grant number: 305/99/0655 and 305/99/0657; Grant sponsor: the Ministry of Education, Youth and Sport of the Czech Republic; Grant number: LN00A065; Grant sponsor: Swedish Cancer Research Foundation; Grant number: 3622; Grant sponsor: the Swedish Medical Research Council; Grant number: 11548; Grant sponsor: the Swedish Society for Medicine; Grant sponsor: Swedish Society for Medical Research; Grant sponsor: the King Gustaf V's Foundation; Grant sponsor: StrokeFond; Grant sponsor: Volvo Assar Gabrielsson's Fond.

*Correspondence to: Eva Syková, Department of Neuroscience, Institute of Experimental Medicine ASCR, Vídeňská 1083, 142 20 Praha 4, Czech Republic. E-mail: sykova@biomed.cas.cz

Received 15 February 2001; Accepted 29 May 2001

al., 1996). These animals reproduce and develop normally, with no obvious anatomic, behavioral, or histological abnormalities, and GFAP deficiency does not cause upregulation of other intermediate filament proteins, such as vimentin or nestin. On the contrary, due to the inability of vimentin to assemble into IFs on its own, the absence of GFAP leads to an absence of intermediate filaments in nonreactive astrocytes in vivo (Pekny et al., 1998a; Eliasson et al., 1999). It was demonstrated that GFAP is not crucial for the morphogenesis of the CNS and that its absence does not have any major effect on the formation of a posttraumatic glial scar (Pekny et al., 1999) or on the cause of prion disease (Gomi et al., 1995; Tatzel et al., 1996). Interestingly, GFAP-deficient mice were found to be more sensitive to percussive head injury with a weight drop device, implying a role for GFAP in the mechanical resistance of brain tissue (Nawashiro et al., 1998). One study showed that $GFAP^{-/-}$ mice displayed enhanced long-term potentiation (LTP) of both population spike amplitude and excitatory postsynaptic potential slope in the hippocampus following tetanic stimulation (McCall et al., 1996), while another report showed normal LTP in GFAP–deficient mice (Shibuki et al., 1996). The study of Shibuki et al. (1996) also indicated that GFAP-negative mice are deficient in long-term depression at distinct sites in the brain as well as in eyeblink conditioning, suggesting modulation of neuronal functions by astrocytes. It was therefore suggested that GFAP is important for astrocyte-neuronal interactions and that astrocytic processes play a vital role in modulating synaptic efficacy in the CNS. It was also demonstrated by Liedtke et al. (1996) that GFAP expression is essential for normal white matter architecture and blood-brain barrier (BBB) integrity in aged mice, and its absence may lead to a late onset of CNS demyelination. A significant decrease in BBB induction by $GFAP^{-/-}$ astrocytes was shown in aortic endothelial cells in vitro (Pekny et al., 1998b). These results suggest that GFAP may play a role in the induction of BBB properties in endothelial cells.

A number of studies have shown that astrocytes regulate the ionic and volume homeostasis of the extracellular space in a wide range of pathological states affecting the central nervous system (CNS), including ischemia, hypoxia, and trauma (Chiang et al., 1968; Bourke et al., 1980; Long, 1981; Kimelberg et al., 1992; Syková et al., 1999). Astrocyte swelling can be evoked by elevated extracellular potassium concentration ($[K^+]_e$) in a perfusing solution or hypo-osmotic saline (Walz, 1989, 1992). Both in vivo and in vitro studies have shown that cell swelling results in a compensatory ECS volume decrease and in alterations of the ECS geometry (Svoboda and Syková, 1991; Syková, 1997; Voříšek and Syková, 1997; Nicholson and Syková, 1998; Syková et al., 1999). Pronounced but transient cell swelling also occurs during pathological states, such as Leao's cortical spreading depression (Leao, 1944), which is characterized by a wave of depolarization propagating slowly over the cerebral cortex, a rise in $[K^+]_e$ up to 60 mM, and suppression of neuronal activity (Bureš et al., 1974). Our previous studies have shown that K^+ accumulation is determined by the ECS volume in the vicinity of the cell and is larger around oligodendrocytes than around astrocytes (Chvátal et al., 1999). It was previously shown that the lack of IFs in reactive astrocytes in vitro following hypotonic stress, a situation resembling hypoxia-induced cytotoxic edema in the brain, leads to diminished taurine release (Ding et al., 1998). This study implied that astrocytic IFs may play a role in volume regulation in situations such as stroke.

In the present study, we examined the role of GFAP during cell swelling, which is accompanied by an ECS volume decrease and by an increase in ECS diffusion barriers, in $GFAP^{+/+}$ and $GFAP^{-/-}$ mice. Astrocyte membrane currents and ECS diffusion parameters were studied in spinal cord slices. A model of spreading depression in the somatosensory cortex was used to study the role of GFAP during cell swelling in pathological states in vivo.

MATERIALS AND METHODS

Spinal Cord Slices

$GFAP^{+/+}$ and $GFAP^{-/-}$ mice (Pekny et al., 1995) were sacrificed under ether anesthesia at postnatal days 8 to 10 (P8–10) by decapitation. Spinal cord slices were prepared as described previously (Chvátal et al., 1995). In brief, spinal cords were dissected and washed in artificial cerebrospinal fluid (ACF) at 8–10°C. A 4–5 mm long segment of the lumbar cord was embedded in 1.7% agar at 37°C (Purified Agar, Oxoid, U.K.). Transverse 200 μm thick slices were made using a vibroslice (752M, Campden Instruments, U.K.) for patch-clamp recording, while for ECS diffusion measurements 400 μm thick slices were used. The recording chamber (~ 2 ml volume) was continuously perfused with oxygenated ACF at the rate of 5 ml/min. All experiments were carried out at room temperature (~22°C).

The artificial cerebrospinal fluid (ACF) contained (in mM): NaCl 117.0, KCl 3.0, $CaCl_2$ 1.5, $MgCl_2$ 1.3, Na_2HPO_4 1.25, $NaHCO_3$ 35.0, D-Glucose 10.0, osmolality 300 mmol/kg. The solution was continuously gassed with a mixture of 95% O_2 and 5% CO_2 to maintain a final pH of 7.4. To keep the solutions iso-osmolar, ACF containing 50 mM K^+ had a reciprocally reduced Na^+ concentration (300 mmol/kg). Hypo-osmotic solution (200 mmol/kg) had a reduced concentration of NaCl (to 69 mM). Osmolality was measured using a vapor pressure osmometer (Vapro 5520, Wescor, Logan).

Animal Preparation for In vivo Measurements

Three- to 6-month-old $GFAP^{+/+}$ and $GFAP^{-/-}$ mice were anesthetized with sodium pentobarbital (90 mg/kg, injected i.p.) and placed in a rat head holder. Mice

were breathing room air spontaneously. Body temperature was maintained with a heating pad at 37°C ± 1°C. One small trephination hole for TMA^+ diffusion measurements was made over the somatosensory cortex. Another opening for eliciting spreading depression (SD) was made 1.5–2 mm caudal to the first hole. During the experiment, the exposed cortex was superfused with ACF containing 1 mM TMA^+ chloride (tetramethylammonium). The solution was warmed to 37°C. SD was evoked by pricking the upper cortical layers with the tip of a 0.5 mm spinal needle (Mazel et al., 2001).

Patch-Clamp Recordings

Glial membrane currents were recorded with the patch-clamp technique in the whole-cell configuration (Hamill et al., 1981). Recording pipettes with a tip resistance of 4–6 MΩ were made from borosilicate capillaries (Rückl Glass, Otvovice, Czech Republic) using a Brown-Flaming micropipette puller (P-97, Sutter Instruments Company, Novato). Electrodes were filled with a solution containing (in mM): KCl 130.0, $CaCl_2$ 0.5, $MgCl_2$ 2.0, EGTA 5.0, HEPES 10.0. The pH was adjusted with KOH to 7.2. The intracellular solution contained 1 mg/ml Lucifer Yellow Dilithium salt (Sigma).

In the spinal cord slices, the cell somata were approached by the patch electrode using an INFRA-PATCH system (Luigs and Neumann, Ratingen, Germany). The slices were placed in a chamber mounted on the stage of a fluorescence microscope (Axioskop FX, Carl Zeiss, Germany) and fixed using a U-shaped platinum wire with a grid of nylon threads (Edwards et al., 1989). Selected cells with a membrane potential more negative than −65 mV (n = 115) had a clear, dark membrane surface and were located 5–10 μm below the slice surface. The cells with membrane potential more positive than −65 mV (n = 4) were located on the surface and were therefore excluded from further analysis, because their processes could have been damaged during the slice preparation. The cells and the recording electrode were imaged with an infrared-sensitive video camera (C2400-03, Hamamatsu Photonics, Hamamatsu City, Japan) and displayed on a standard TV/video monitor. Current signals were amplified with an EPC-9 amplifier (HEKA Elektronik, Lambrecht/Pfalz, Germany), lowpass-filtered at 3 kHz and sampled at 5 kHz by an interface connected to an AT-compatible computer system, which also served as a stimulus generator. Data acquisition, storage, and analysis were performed with TIDA (HEKA Elektronik).

Membrane potential (V_m) was measured by switching the EPC-9 amplifier to the current clamp mode. Two stimulation paradigms were used to activate membrane currents. To distinguish between glial cell types, the cell membrane was clamped from the holding potential of −70 mV to values ranging from −160 mV to +20 mV at intervals of 10 mV. For tail current analysis, the glial membrane was first briefly depolarized using a prepulse with an amplitude of 90 mV, i.e., by changing the holding potential from −70 mV to +20 mV for 20 ms (Fig. 1A–C). After the depolarizing prepulse, a series of 20 ms de- and hyperpolarizing pulses ranging from −130 mV to +20 mV was applied. The reversal potential (V_{rev}) of tail currents (I_{tail}) was determined from the current/voltage (I/V) relationship measured 5 ms after the offset of the depolarizing prepulse.

Measurements of Extracellular Space Diffusion Parameters

The real-time iontophoretic method was used to determine ECS diffusion parameters, namely volume fraction α (ECS volume/total tissue volume), tortuosity λ (λ^2 = free/apparent diffusion coefficient), and nonspecific cellular uptake k′ (nonspecific TMA^+ uptake characterizing the clearance of TMA^+ from the ECS), in the ECS of the spinal cord slice gray matter and cortex in vivo (Nicholson and Phillips, 1981; Nicholson and Syková, 1998). In brief, a substance to which cell membranes are relatively impermeable, i.e., TMA^+, was administered using an iontophoretic electrode into the ECS of the nervous tissue. Iontophoretic electrodes were made from theta glass tubing (Clark Electromedical Instruments, England) and filled with 100 mM TMA^+. The concentration of TMA^+ was then measured by means of a double-barreled TMA^+-sensitive microelectrode (TMA^+-ISM) at a fixed distance from the tip of the iontophoretic electrode. TMA^+-ISMs were prepared by a procedure described previously (Syková et al., 1994). The ion exchanger was Corning 477317 and the ion-sensitive barrel was back-filled with 100 mM TMA^+ chloride. The reference barrel contained 150 mM NaCl. Electrodes were calibrated using the fixed-interference method before and after each experiment in a sequence of solutions containing increasing concentrations of TMA^+. Each calibration was fitted to the Nikolsky equation to determine electrode slope and interference (Nicholson and Philips, 1981). The shank of the iontophoretic electrode was bent so that it could be aligned parallel to the TMA^+-ISM. Both TMA^+-ISM and iontophoretic electrodes were glued together using dental cement with an intertip distance of 120–200 μm (Fig. 1D and E). To calibrate the microelectrode array, TMA^+ diffusion curves were first recorded in 0.3% agar (Special Noble Agar, Difco, Detroit, MI) dissolved in a solution containing 150 mM NaCl, 3 mM KCl, and 1 mM TMACl. Typical iontophoretic parameters were +20 nA bias current continuously applied to keep a constant transport number of the iontophoretic electrode with an +80 nA current step of 60 s duration applied every 3–5 min to generate a diffusion curve. The microelectrode array was then lowered into the spinal cord slice, perfused with ACF containing 0.1 mM TMACl, to a depth of 200 μm or into the brain cortex to

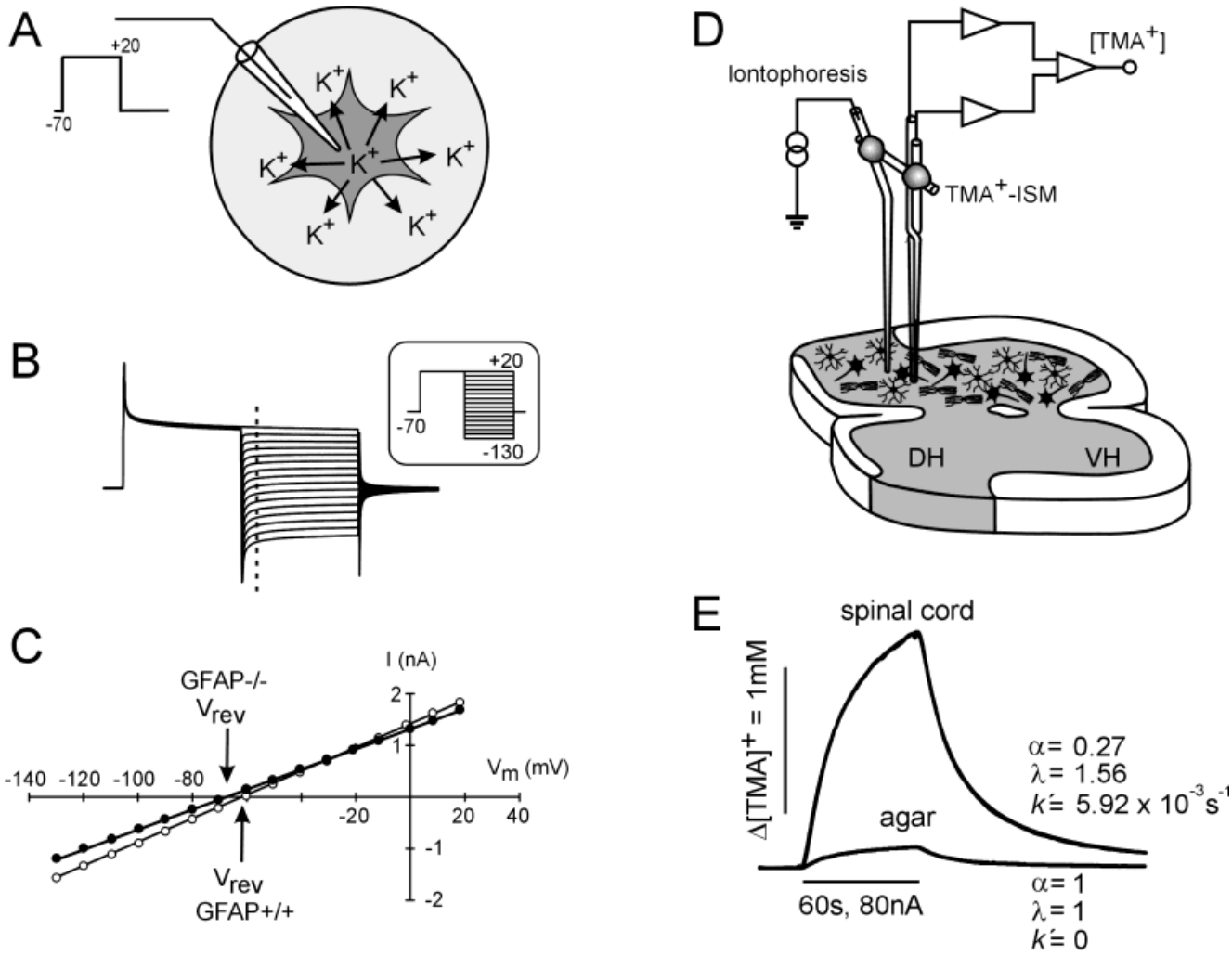

Fig. 1. Tail current analysis in astrocytes (**A**–**C**) and ECS diffusion parameters measurements in GFAP$^{+/+}$ and GFAP$^{-/-}$ mouse spinal cord slices (**D** and **E**). For the tail current analysis, the membranes of astrocytes were clamped from a holding potential of −70 mV to +20 mV for 20 ms, which triggered an efflux of K^+ from the astrocyte into the vicinity of the astrocyte membrane (A). After this prepulse, the membrane was clamped for 20 ms to increasing de- and hyperpolarizing potentials (pattern of voltage commands in inset) ranging from −130 mV to +20 mV, at 10 mV increments (B). From traces as shown in B, currents (I) were measured 5 ms after the onset of the de- and hyperpolarizing pulses (dashed line) and plotted as a function of the membrane potential (V_m). The reversal potentials (V_{rev}) in GFAP$^{+/+}$ and GFAP$^{-/-}$ astrocytes are indicated in the graphs by arrows (C). Experimental setup of the real-time TMA^+ iontophoretic method (D) and a typical diffusion curve of TMA^+ in the gray matter of a mouse spinal cord slice (E). TMA^+ was administered into the gray matter of the spinal cord slice using an iontophoretic electrode (D). The concentration of TMA^+ was then measured in the ECS by means of a double-barreled TMA^+-sensitive microelectrode (ISM). TMA^+-ISM and iontophoretic electrodes were glued together and lowered into the gray matter of the spinal cord slice with an intertip distance of 120–200 μm. The diffusion curves obtained from the spinal cord slices were analyzed by fitting the data to a solution of a modified diffusion equation to yield the diffusion parameters of the spinal cord nervous tissue, namely volume fraction α and tortuosity λ (E).

a depth of 400 μm. The diffusion curves were recorded with a PC-based computer and analyzed by fitting the data to a solution of a modified diffusion equation (Nicholson and Phillips, 1981) to yield the diffusion parameters α, λ, and k′ (Fig. 1E).

Cell Morphology and Immunohistochemistry

During electrophysiological measurements cells were filled with Lucifer Yellow by dialyzing the cytoplasm with the patch pipette solution. The morphology of Lucifer Yellow (LY)-filled cells was studied in an unfixed spinal cord slice using a fluorescence microscope (Axioskop, Zeiss) equipped with a fluorescein isothiocyanate filter combination (band pass 450–490 nm, mirror 510 nm, long pass 520 nm).

For immunohistochemical analysis, 200 μm spinal cord slices with LY-injected cells were fixed with 4% paraformaldehyde in 0.1 M phosphate-buffer (PB; pH 7.5) for 4 h, washed and kept in 0.1 M PB. GFAP$^{+/+}$ astrocytes were identified using a mouse monoclonal antibody against GFAP coupled to Cy3 (Sigma). GFAP antibodies were diluted 1:200 in PB saline (PBS) con-

taining 1% bovine serum albumin (BSA; Sigma) and 0.5% Triton X-100 (Sigma). After overnight incubation, the slices were visualized using a fluorescence microscope equipped with filters 09 (Axioplan 2, Zeiss, band pass 450–490 nm for LY-injected cells) and 15 (Zeiss, H 546 for GFAP immunostaining).

To quantify morphological differences between GFAP$^{+/+}$ and GFAP$^{-/-}$ astrocytes, the spectral confocal microscope LEICA TCS SP system equipped with Arg/HeNe lasers was used. The number and thickness of processes were determined from the intensity profiles measured in three circles situated 20, 40, and 60 μm from the center of cell soma. The number of glial processes corresponded to the number of peaks in the xy intensity profile exceeding a threshold value of 50 on the 0–250 gray scale. The width of each process was determined from the corresponding width of the intensity profile peak at a distance of 40 μm from the center of cell soma. The height of each peak was divided in half and its width was taken at this point (Fig. 2).

Statistical Analysis

Results are expressed as mean ± SEM. Statistical analysis of the differences between groups was evaluated using a *t*-test. Values of $P < 0.05$ were considered significant.

RESULTS

Morphology of GFAP$^{+/+}$ and GFAP$^{-/-}$ Astrocytes

Mouse spinal cord astrocytes were identified on the basis of previously described electrophysiological and morphological properties typical for rat spinal cord astrocytes (Chvátal et al., 1995, 1999; Pastor et al., 1995). Immunohistochemical analysis of glial cells in GFAP$^{+/+}$ mice confirmed that two out of eight glial cells with passive, symmetrical, and nondecaying K^+ conductance showed positive staining when tested with anti-GFAP antibody (Chvátal et al., 1995), and therefore glial cells with passive K^+ conductance were considered to be astrocytes in both wild-type and knockout animals (Fig. 3).

As revealed by LY fluorescence, astrocytes in unfixed spinal cord slices were characterized by round or elliptical cell bodies 10–15 μm in diameter with very fine processes, which formed a diffuse network around the cell. Morphological analysis of 23 astrocytes from GFAP$^{+/+}$ mice revealed that about 74% of cells (n = 17) were characterized by multiple, long, branched processes that exceeded a 60 μm radius from the center of the cell soma; 26% of astrocytes (n = 6) exhibited only short processes with less branching, not exceeding a 60 μm radius from the center of the cell soma. In contrast to GFAP$^{+/+}$ astrocytes, 63% of GFAP$^{-/-}$ astrocytes (n = 22) had short processes with less branching and only 37% of astrocytes (n = 13) had long processes with branching similar to that observed in GFAP$^{+/+}$ astrocytes. Analysis of astrocyte morphology using confocal microscopy and quantification of xy intensity profiles in a confocal plane revealed a lower density of processes in GFAP$^{-/-}$ astrocytes than in GFAP$^{+/+}$ astrocytes (Fig. 2A and B). In GFAP$^{+/+}$ astrocytes, the number of processes measured 20 and 40 μm from the center of the cell soma was 34 ± 3 and 16 ± 2, respectively (n = 7). In GFAP$^{-/-}$ astrocytes, the number of processes was significantly lower, 20 ± 2 and 10 ± 1, respectively (n = 8). The number of processes at 60 μm was not significantly different, 7 ± 1 in GFAP$^{+/+}$ and 4 ± 1 in GFAP$^{-/-}$ astrocytes. The width of processes measured 40 μm from the center of cell soma was significantly smaller in GFAP$^{-/-}$ astrocytes (0.47 ± 0.01 μm; n = 43) than in GFAP$^{+/+}$ astrocytes (0.52 ± 0.02 μm; n = 30, Fig. 2C). The number of dye-coupled astrocytes in GFAP$^{+/+}$ and GFAP$^{-/-}$ mice was not significantly different; 21% of GFAP$^{+/+}$ and 17% of GFAP$^{-/-}$ astrocytes were dye-coupled to another cell.

Membrane Properties of GFAP$^{+/+}$ and GFAP$^{-/-}$ Astrocytes

Patch-clamp recordings were made from astrocytes located in the dorsal horn gray matter of GFAP$^{+/+}$ and GFAP$^{-/-}$ mice. The following membrane properties were compared: membrane potential (V_m), membrane currents activated by de- or hyperpolarizing voltage steps, and reversal potential (V_{rev}) of the tail currents (I_{tail}) observed after the offset of the de- or hyperpolarizing prepulse.

Both GFAP$^{+/+}$ and GFAP$^{-/-}$ astrocytes were characterized by similar large, symmetrical outward and inward, nondecaying K^+-selective currents during the voltage jump (Fig. 3A and B). Table 1 shows that no significant differences were observed between the V_m of GFAP$^{+/+}$ and GFAP$^{-/-}$ astrocytes. In addition, we found no differences in the amplitude of the outward (I_{out}) or inward (I_{in}) currents evoked by de- and hyperpolarizing pulses measured at the end of the 50 ms voltage pulse. K^+ accumulation in the vicinity of the glial membrane was studied using tail current analysis after the depolarizing prepulse (Chvátal et al., 1999). V_{rev} of I_{tail} in GFAP$^{+/+}$ astrocytes was about −63 mV, while V_{rev} of I_{tail} in GFAP$^{-/-}$ astrocytes was more negative, i.e., about −66 mV (Table 1). Since the astrocytic membrane is almost exclusively permeable to K^+, the V_{rev} of the membrane may be calculated using the Nernst equation $V_{rev} = V_m = (RT/F)\ln([K^+]_e/[K^+]_i)$ (Kuffler et al., 1966; Berger et al., 1991; Chvátal et al., 1997). The extracellular K^+ concentrations before ($[K^+{}_m]_e$) and after the depolarizing prepulse ($[K^+{}_{rev}]_e$) were therefore calculated using the Nernst equation from the corresponding values of V_m and V_{rev} of I_{tail}. The net increase in $[K^+]_e$ ($\Delta[K^+]_e$) induced by a depolarizing prepulse was determined by subtracting the values of $[K^+{}_m]_e$ from $[K^+{}_{rev}]_e$ (Chvátal et al., 1999). In GFAP$^{+/+}$ astrocytes, the mean increase in $[K^+]_e$ in-

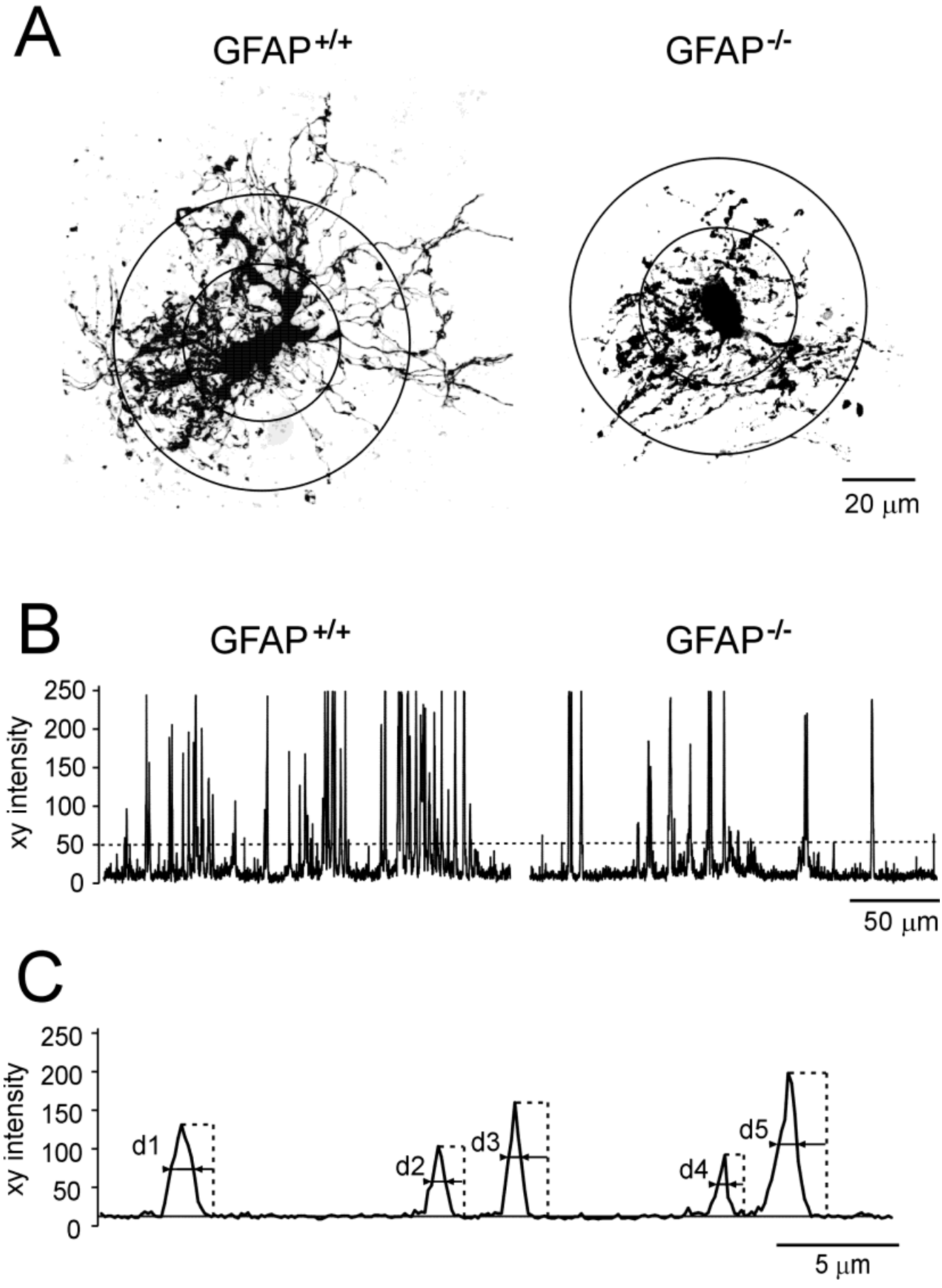
A
GFAP+/+
GFAP-/-
20 μm
B
GFAP+/+
GFAP-/-
xy intensity
250
200
150
100
50
0
50 μm
C
xy intensity
250
200
150
100
50
0
d1
d2
d3
d4
d5
5 μm

Figure 2.

duced by a depolarizing prepulse was 4.85 mM, while in GFAP$^{-/-}$ astrocytes, the increase was significantly smaller, i.e., 3.37 mM (Table 1), suggesting the presence of a larger ECS in the vicinity of GFAP$^{-/-}$ astrocytes.

Effect of 50 mM K^+ and Hypotonic Solution on Membrane Properties of GFAP$^{+/+}$ and GFAP$^{-/-}$ Astrocytes

The effect of astrocytic swelling on extracellular K^+ accumulation evoked by a depolarizing prepulse was studied during superfusion of the spinal cord slice either with an iso-osmotic solution containing 50 mM K^+ or with a hypotonic solution with reduced NaCl (200 mmol/kg). V_m and V_{rev} of I_{tail} in GFAP$^{+/+}$ and GFAP$^{-/-}$ astrocytes were measured at 2-min intervals before, during, and after the application of 50 mM K^+ or hypotonic solution.

Astrocyte swelling induced by a 20-min perfusion of the spinal cord slice in 50 mM K^+ shifted the V_m and V_{rev} of I_{tail} in both GFAP$^{+/+}$ and GFAP$^{-/-}$ astrocytes to more positive values (Fig. 4A and C) without any significant differences. In GFAP$^{+/+}$ astrocytes, V_m changed from -75.83 ± 0.40 mV to -18.45 ± 0.45 mV ($n = 5$) and in GFAP$^{-/-}$ astrocytes from -76.40 ± 1.03 to -17.78 ± 0.56 mV ($n = 7$). V_{rev} of I_{tail} shifted from -59.73 ± 1.88 mV to -10.68 ± 1.99 mV in GFAP$^{+/+}$ astrocytes and from -64.64 ± 1.65 mV to -15.77 ± 0.32 mV in GFAP$^{-/-}$ astrocytes. However, $[K^+]_e$ changes calculated from the Nernst equation revealed a smaller accumulation of K^+ induced by a depolarizing prepulse in the vicinity of GFAP$^{-/-}$ astrocytes than in the vicinity of GFAP$^{+/+}$ astrocytes (Fig. 4B and D). During the application of 50 mM K^+, $\Delta[K^+]_e$ increased in GFAP$^{+/+}$ astrocytes from 5.92 ± 0.79 to 23.80 ± 7.00 mM, while in GFAP$^{-/-}$ astrocytes $\Delta[K^+]_e$ increased only from 3.81 ± 0.89 to 6.53 ± 0.96 mM. When the application of 50 mM K^+ was discontinued, V_m and V_{rev} of I_{tail} slowly returned toward control values, showing no significant differences in K^+ accumulation between GFAP$^{+/+}$ and GFAP$^{-/-}$ astrocytes. Twenty minutes after 50 mM K^+ washout, $\Delta[K^+]_e$ around GFAP$^{+/+}$ and GFAP$^{-/-}$ astrocytes was 4.04 ± 0.93 mM and 4.40 ± 0.58 mM, respectively.

During cell swelling induced by hypotonic solution, V_m of GFAP$^{+/+}$ and GFAP$^{-/-}$ astrocytes shifted to more negative values, while V_{rev} of I_{tail} shifted to more positive values (Fig. 5A and C). In both GFAP$^{+/+}$ and GFAP$^{-/-}$ astrocytes, the maximal change of V_m was observed approximately 4 min after the onset of superfusion with hypotonic solution, reaching values of about -83 mV and -86 mV, respectively. During a 20-min application of HS, V_m returned toward control values. V_m changed from -75.6 ± 1.25 mV to -76.6 ± 0.75 mV ($n = 5$) in GFAP$^{+/+}$ astrocytes and from -78.64 ± 1.50 mV to -78.68 ± 1.87 mV ($n = 7$) in GFAP$^{-/-}$ astrocytes. In contrast to V_m, a significant shift in V_{rev} of I_{tail} was observed. In GFAP$^{+/+}$ astrocytes, it changed from -59.92 ± 1.80 mV to -35.73 ± 1.43 mV and in GFAP$^{-/-}$ astrocytes from -64.87 ± 2.84 mV to -46.53 ± 4.04 mV. Similarly to astrocyte swelling evoked by 50 mM K^+, the net increase in K^+ in the vicinity of the cell induced by a depolarizing prepulse was smaller in GFAP$^{-/-}$ than in GFAP$^{+/+}$ astrocytes (Fig. 5B and D). During the application of hypotonic solution, $\Delta[K^+]_e$ in GFAP$^{+/+}$ astrocytes increased from 5.71 ± 1.03 mM to 25.52 ± 1.73 mM, while in GFAP$^{-/-}$ astrocytes it increased only from 4.51 ± 0.94 mM to 16.24 ± 3.02 mM. When the hypotonic solution was replaced with normal ACF, V_m slowly returned to control values, while V_{rev} of I_{tail} remained increased in both GFAP$^{+/+}$ and GFAP$^{-/-}$ astrocytes; therefore, $\Delta[K^+]_e$ remained increased at 7.82 ± 1.12 mM and 6.98 ± 0.97 mM, respectively.

Effect of 50 mM K^+ and Hypotonic Solution on ECS Diffusion Parameters

Three ECS diffusion parameters (volume fraction α, tortuosity λ, and nonspecific cellular uptake k') were determined in the spinal dorsal horn of GFAP$^{+/+}$ and GFAP$^{-/-}$ mice. In ACF, the mean values of the ECS diffusion parameters were similar in GFAP$^{+/+}$ and GFAP$^{-/-}$mice, $\alpha = 0.27$–0.28 and $\lambda = 1.55$ (Table 2).

The application of 50 mM K^+ or hypotonic solution had a different effect in GFAP$^{+/+}$ and GFAP$^{-/-}$ animals (Fig. 6, Table 2). In GFAP$^{+/+}$ mice, 50 mM K^+ led to a decrease in ECS volume ($\alpha = 0.07$), to an increase in λ to about 1.92, and to an increase in k' (8.94×10^{-1} s^{-3}). In GFAP$^{-/-}$ mice, the changes in ECS diffusion parameters were significantly smaller than in GFAP$^{+/+}$ mice: α decreased to 0.12, λ increased to 1.72, and k' only increased to 6.99×10^{-3} s^{-1} (Fig. 6A and C; Table 2). As compared to GFAP$^{+/+}$ mice, the decrease in α was substantially slower in GFAP$^{-/-}$ mice. After superfusion of the spinal cord slice with normal ACF, α, λ, and k' returned toward control values.

The application of a hypotonic solution (200 mmol/kg) for 20 min also had different effects on ECS diffusion parameters in GFAP$^{+/+}$ and GFAP$^{-/-}$ animals (Fig. 6B and D; Table 2). In GFAP$^{+/+}$ mice, α decreased to 0.12, λ increased to 1.63, and k' increased to 8.58×10^{-3} s^{-1}, while in GFAP$^{-/-}$ mice α decreased to only

Fig. 2. Morphology and intensity profile of processes in GFAP$^{+/+}$ and GFAP$^{-/-}$ astrocytes. Typical morphology of GFAP$^{+/+}$ astrocyte (left) and GFAP$^{-/-}$ astrocyte (right) with circles at 20 μm and 40 μm from the center of the cell soma (**A**). The number and the width of astrocyte processes were quantified using a spectral confocal microscope (see text). Number of processes is expressed as the number of peaks in the xy intensity profile measured at 40 μm from the center of the cell soma. An intensity of 50 on the 0–250 gray scale was taken as the threshold (**B**). The width of each process was determined at a distance of 40 μm from the center of the cell body from the corresponding width of the intensity profile peak. The height of each peak was divided in half and its width was measured at this point (**C**). The trace in C shows an example of five intensity profile peaks (d1–d5) that correspond to five astrocyte processes.

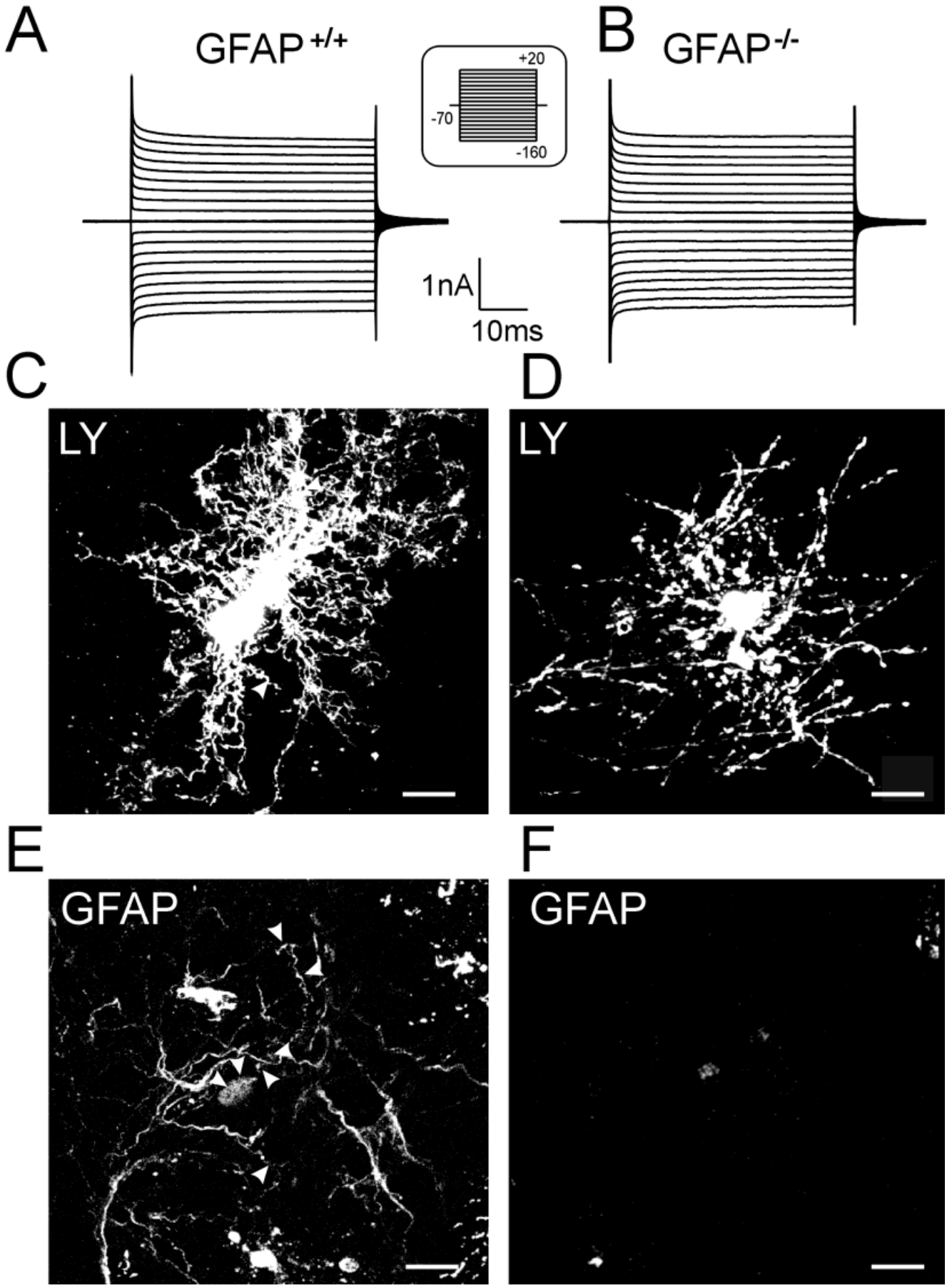

Figure 3.

*TABLE 1. Electrophysiological Parameters of GFAP$^{+/+}$ and GFAP$^{-/-}$ Astrocytes in Mouse Spinal Cord Slices**

		GFAP$^{+/+}$	GFAP$^{-/-}$
V_m	[mV]	−77.46 ± 0.59	−76.62 ± 0.52
K_m^+	[mM]	6.13 ± 0.14	6.32 ± 0.13
V_{rev}	[mV]	−63.48 ± 1.10	−66.27 ± 0.81[a]
K_r^+	[mM]	10.98 ± 0.48	9.70 ± 0.31[a]
$\Delta[K^+]_e$	[mM]	4.85 ± 0.42	3.37 ± 0.27[b]
I_{out}	[nA]	1.86 ± 0.16	1.77 ± 0.14
I_{in}	[nA]	1.77 ± 0.16	1.75 ± 0.14
n		55	56

*V_m, membrane potential; K_m^+, extracellular K^+ concentration calculated from the values of V_m; V_{rev}, reversal potential of the tail current; K_r^+, extracellular K^+ concentration calculated from the value of V_{rev}; $\Delta[K^+]_e = K_r^+ - K_m^+$; I_{in}, inward current evoked by hyperpolarization; I_{out}, outward currents evoked by depolarization; n, number of measurements. Statistical significance was evaluated as the difference between GFAP$^{+/+}$ and GFAP$^{-/-}$ mice (two-tail t-test).
[a]$P < 0.05$.
[b]$P < 0.01$.

0.16, λ increased to 1.66, and k′ increased to 11.26 × 10^{-3} s^{-1}. Beside differences in α, we also noted differences in the recovery of α and λ to control values (Fig. 6D). In GFAP$^{+/+}$ mice, λ and k′ quickly returned to their original values and α only slightly overshot the control values, while in GFAP$^{-/-}$ mice, α overshot the control values up to 0.41 and λ did not return to control values. Our data show that the changes in ECS diffusion parameters induced by cell swelling in 50 mM K^+ or in hypotonic solution are smaller and slower in GFAP$^{-/-}$ than in GFAP$^{+/+}$ mice. This suggests that cell volume regulation is more efficient in GFAP$^{+/+}$ astrocytes.

ECS Diffusion Parameters During Spreading Depression in Cortex of GFAP$^{+/+}$ and GFAP$^{-/-}$ Mice

ECS diffusion parameters were measured in vivo in the cerebral cortex of GFAP$^{+/+}$ and GFAP$^{-/-}$ mice 3–6 months old. The ECS diffusion parameters were first compared under resting conditions. The mean values of the ECS diffusion parameters in mice differed from those described in the rat cortex: both α and λ were higher (Nicholson and Syková, 1998). In the cortex of GFAP$^{+/+}$ mice, the diffusion parameters were α = 0.24, λ = 1.71, and k′ = 4.0 × 10^{-3} s^{-1}, while in GFAP$^{-/-}$ mice they were α = 0.23, λ = 1.62, and k′ = 4.0 × 10^{-3} s^{-1}. Tortuosity in GFAP$^{+/+}$ mice was significantly higher than in GFAP$^{-/-}$ mice.

The changes in ECS diffusion parameters during spreading depression, elicited by fine-needle pricking of the cortex, also revealed differences between GFAP$^{+/+}$ and GFAP$^{-/-}$ mice. For the measurement of ECS diffusion parameters during SD, at the time of maximal change we used microelectrode arrays with a smaller intertip distance (50–100 μm) and shorter diffusion times (current step duration of 6 s). We found no significant differences in the volume fraction and tortuosity obtained using either a 60-s or 6-s current step. Only the nonspecific TMA^+ uptake was higher when using a 6-s application. SD led to a decrease in α to 0.04 in GFAP$^{+/+}$ and to 0.08 in GFAP$^{-/-}$ mice, λ increased to 2.18 in GFAP$^{+/+}$ and to 1.97 in GFAP$^{-/-}$ mice (Fig. 7A, Table 3). The shrinkage of ECS led to a rapid increase in the TMA^+ baseline concentration (Fig. 7B). The time course of α and λ changes was almost two times slower in GFAP$^{-/-}$ mice (150 ± 20 s) than in GFAP$^{+/+}$ mice (88 ± 13 s, Fig. 7B). Our results show that the changes in ECS diffusion parameters induced by cell swelling during SD are slower in GFAP$^{-/-}$ than in GFAP$^{+/+}$ mice.

DISCUSSION

In the present study performed on spinal cord gray matter of GFAP$^{+/+}$ and GFAP$^{-/-}$ mice, we have shown that the majority of GFAP$^{-/-}$ astrocytes filled with Lucifer Yellow have shorter and thinner processes in comparison to GFAP$^{+/+}$ astrocytes. Our data suggest that K^+ accumulates less in the close vicinity of the cell membrane around GFAP$^{-/-}$ astrocytes after a depolarizing prepulse under resting conditions than it does around GFAP$^{+/+}$ astrocytes. Similar differences in K^+ accumulation were found during cell swelling evoked by 50 mM K^+ or hypotonic solution. Under resting conditions, the ECS diffusion parameters of spinal cord gray matter in GFAP$^{+/+}$ and GFAP$^{-/-}$ mice are similar; however, their changes during cell swelling evoked by high K^+ or hypotonic stress are slower in GFAP$^{-/-}$ mice.

Identification of Astrocytes

In our experiments, astrocytes in GFAP$^{+/+}$ as well as in GFAP$^{-/-}$ mice were characterized by symmetrical nondecaying inward and outward currents in response to de- and hyperpolarizing voltage steps (Chvátal et al., 1995; Pastor et al., 1995). Two out of eight cells (25%) previously characterized electrophysiologically in GFAP$^{+/+}$ mice were identified as astrocytes by positive immunostaining with anti-GFAP antibodies. In the rat spinal cord, the number of cells positively stained with anti-GFAP antibodies was 14% (Chvátal et al., 1995). Such a small percentage of successfully stained cells is not surprising, since it was shown by Ludwin et al. (1976) that intact astrocytes located in the gray matter of the CNS stain for GFAP less intensely than those in

Fig. 3. Typical membrane current patterns of GFAP$^{+/+}$ and GFAP$^{-/-}$ astrocytes (**A** and **B**), morphology (**C** and **D**), and immunostaining of astrocytes for GFAP (**E** and **F**) in GFAP$^{+/+}$ and GFAP$^{-/-}$ mice spinal cord slices. Typical membrane currents of astrocytes recorded in response to voltage steps from a holding potential of −70 mV (A and B). To activate currents, the membrane was clamped for 50 ms from the holding potential of −70 mV to increasing de- and hyperpolarizing potentials ranging from −160 to +20 mV, at 10 mV increments. During the electrophysiological recording, the cell was filled with Lucifer Yellow and then examined with a confocal microscope (C and D). Lucifer Yellow injected cells shown in C and D were immunostained for GFAP (E and F). Arrows indicate similar patterns in both images. Bars in C, D, E, and F denote 10 μm.

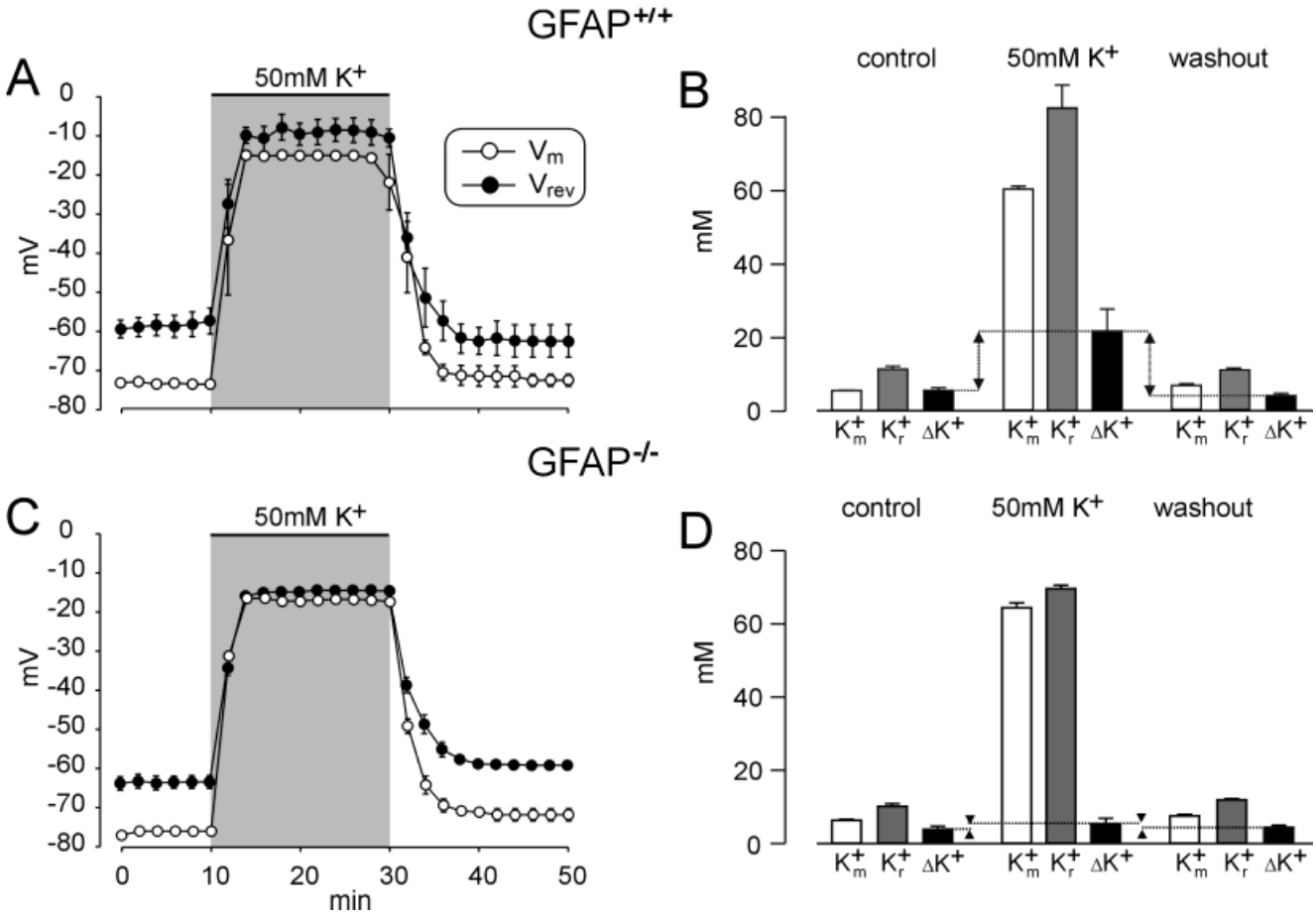

Fig. 4. The effect of 50 mM K^+ on the membrane potential and reversal potential of tail currents in $GFAP^{+/+}$ (**A** and **B**) and $GFAP^{-/-}$ (**C** and **D**) astrocytes. The time course of membrane potentials (V_m, open circles) and reversal potentials of the tail currents (V_{rev}, circles) in $GFAP^{+/+}$ and $GFAP^{-/-}$ astrocytes before, during, and after exposure of the spinal cord slice to 50 mM K^+ (A and C). Using the Nernst equation, $[K^+]_e$ was calculated from the values of V_m (K^+_m) and V_{rev} (K^+_r) and their difference, which is equal to the net increase in $[K^+]_e$ after a depolarizing prepulse $\Delta K^+ = K^+_r - K^+_m$ (B and D).

the white matter. In addition, diluting the intracellular contents of astrocytes with artificial intracellular solution via the patch electrode during electrophysiological recordings may decrease the immunoreactivity of GFAP due to possible conformational changes.

Morphology of $GFAP^{-/-}$ Astrocytes Is Affected by Lack of GFAP

The morphology of astrocytes in $GFAP^{-/-}$ mice was not evaluated in previous studies performed in vivo or in situ because the identification of astrocytes was difficult in the absence of their specific marker, GFAP. In our experiments performed on spinal cord slices, astrocytes were filled with fluorescent dye LY and thus could be visualized. The appearance of astrocytes with a reduced number of thinner processes in $GFAP^{-/-}$ mice is consistent with a smaller accumulation of K^+ around the astrocytes after a depolarizing prepulse. It is also in agreement with the previously observed reduction in cross-sectional diameter of astrocytes lacking GFAP in the optic nerve (McCall et al., 1996). In our study, we cannot exclude the possibility that $GFAP^{-/-}$ astrocyte processes with a small diameter were not sufficiently visualized with LY. However, a direct role for GFAP in controlling the outgrowth of astrocyte processes has been suggested in a number of studies (Weinstein et al., 1991; Rutka and Smith, 1993; Chen and Liem, 1994; Rutka et al., 1994), albeit not confirmed by using in vitro cocultures of neurons and $GFAP^{-/-}$ astrocytes (Pekny et al., 1998a). We can therefore conclude that GFAP, as a structural protein, affects the morphology of astrocytes in the mouse spinal cord, particularly the number and width of processes.

Membrane Properties of $GFAP^{-/-}$ Astrocytes and ECS Diffusion Parameters in Spinal Cord Gray Matter Under Resting Conditions

We found that membrane potential, current pattern, and membrane conductance, as revealed by the behavior of inward and outward currents evoked by hyper- or

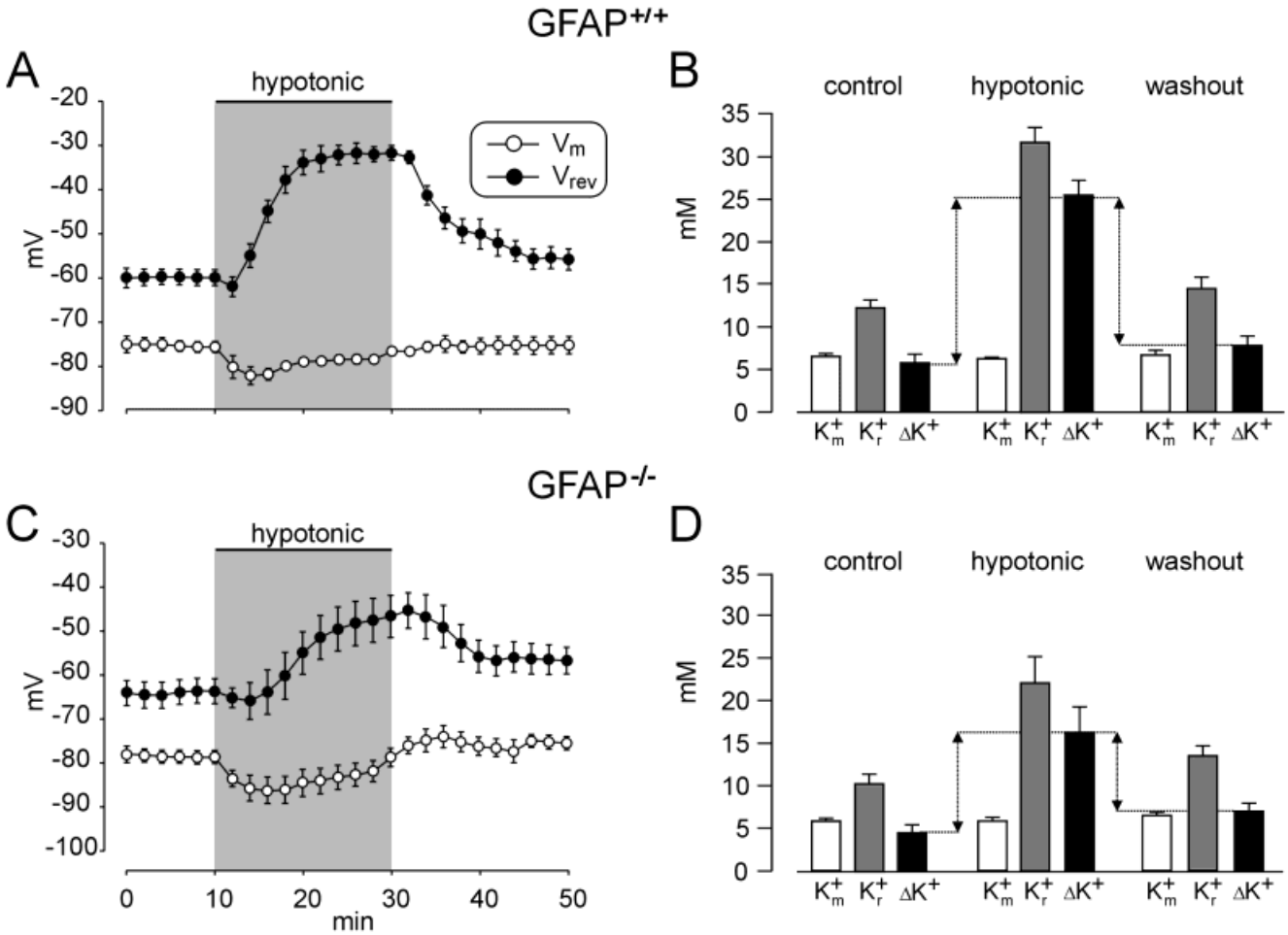

Fig. 5. The effect of hypotonic solution on the membrane potential and reversal potential of tail currents in GFAP$^{+/+}$ (**A** and **B**) and GFAP$^{-/-}$ astrocytes (**C** and **D**). The time course of membrane potentials (V_m, open circles) and reversal potentials of the tail currents (V_{rev}, circles) before, during, and after the application of hypotonic solution (A and C). Using the Nernst equation, $[K^+]_e$ was calculated from the values of V_m (K^+_m) and V_{rev} (K^+_r) and their difference, which is equal to the net increase in $[K^+]_e$ after a depolarizing prepulse $\Delta K^+ = K^+_r - K^+_m$ (B and D).

depolarization stimuli, of GFAP$^{-/-}$ and GFAP$^{+/+}$ astrocytes are similar. Both types of astrocytes show typical symmetrical, passive, and nondecaying K^+-selective currents, similar to those observed in the rat and frog spinal cord slices and mouse cerebellum (Chvátal et al., 1995, 2001; Pastor et al., 1995; Chvátal and Syková, 2000).

It was shown by Orkand et al. (1966) that the astrocytic membrane is almost exclusively permeable to K^+. Previous studies revealed that depolarization of the glial membrane evokes an efflux of K^+ into the ECS and that K^+ accumulation depends on the ECS volume in the vicinity of the cell (Berger et al., 1991; Chvátal et al., 1997, 1999; Chvátal and Syková, 2000). $[K^+]_e$ was calculated from V_{rev} of I_{tail} using the Nernst equation. We did not consider K^+ gradients inside the cells, changes in $[K^+]_i$ (Kettenmann et al., 1983), or the permeability of astrocyte membranes for other ions under resting conditions (Ballanyi et al., 1987; Lascola et al., 1996, 1998), because their contribution to the estimate of $[K^+]_e$ is

*TABLE 2. Values of α, λ, and k′ During a 20-min Application of 50 mM K^+ or Hypotonic Solution in the Gray Matter of Spinal Cord Slices of GFAP$^{+/+}$ and GFAP$^{-/-}$ Mice**

	Control	50 mM K^+	Hypotonic
GFAP$^{+/+}$			
α	0.27 ± 0.01	0.07 ± 0.01[a]	0.12 ± 0.01[a]
λ	1.54 ± 0.02	1.92 ± 0.03[a]	1.63 ± 0.01[b]
k′	5.41 ± 0.74	8.94 ± 0.60[b]	8.58 ± 0.56[c]
n	10	5	5
GFAP$^{-/-}$			
α	0.28 ± 0.01	0.12 ± 0.01[a,d]	0.16 ± 0.01[a,c]
λ	1.55 ± 0.02	1.72 ± 0.04[b,d]	1.66 ± 0.02[b]
k′	6.31 ± 0.87	6.99 ± 2.00	11.26 ± 1.45[b]
n	9	5	5

*The values of extracellular volume fraction α, tortuosity λ, and nonspecific uptake k′ ($\times 10^{-3}$ s^{-1}) before (control) and at the time of maximal change evoked by the application of 50 mM K^+ or hypotonic solution (200 mmol/kg) in GFAP$^{+/+}$ and GFAP$^{-/-}$ mice. Statistical significance was evaluated as the difference between GFAP$^{+/+}$ and GFAP$^{-/-}$ mice (d and e, unpaired, two-tailed *t*-test) and as the difference between ACF and either 50 mM K^+ or hypotonic solution (a, b, and c, unpaired, two-tailed *t*-test).
[a] $P < 0.0001$.
[b] $P < 0.01$.
[c] $P < 0.05$.
[d] $P < 0.005$.
[e] $P < 0.05$.

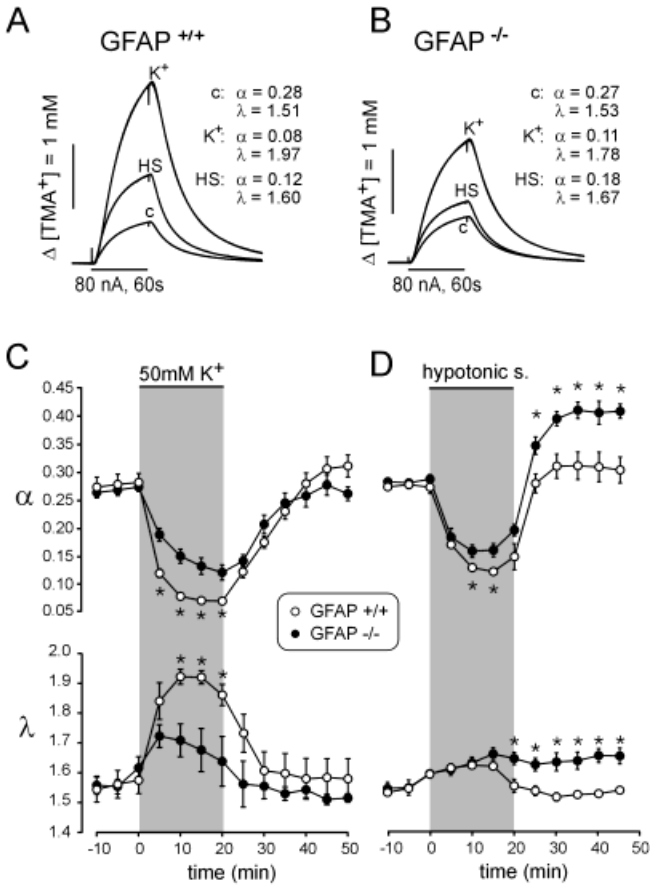

Fig. 6. Typical diffusion curves (**A** and **B**) and the time course of changes in volume fraction (α) and tortuosity (λ) during the application of 50 mM K^+ (**C**) and hypotonic solution (**D**) in dorsal horn gray matter of spinal cord slices of 8- to 10-day-old $GFAP^{+/+}$ and $GFAP^{-/-}$ mice. The normalized diffusion curves obtained in ACF (c) and at the time of maximal changes evoked by the application of 50 mM K^+ (K^+) or hypotonic solution (HS) are shown with the corresponding values of α and λ (A and B). Each data point of α and λ was recorded at 5-min intervals before, during, and after the application of 50 mM K^+ (C) and hypotonic solution (D). Stars indicate significant difference of $P < 0.05$.

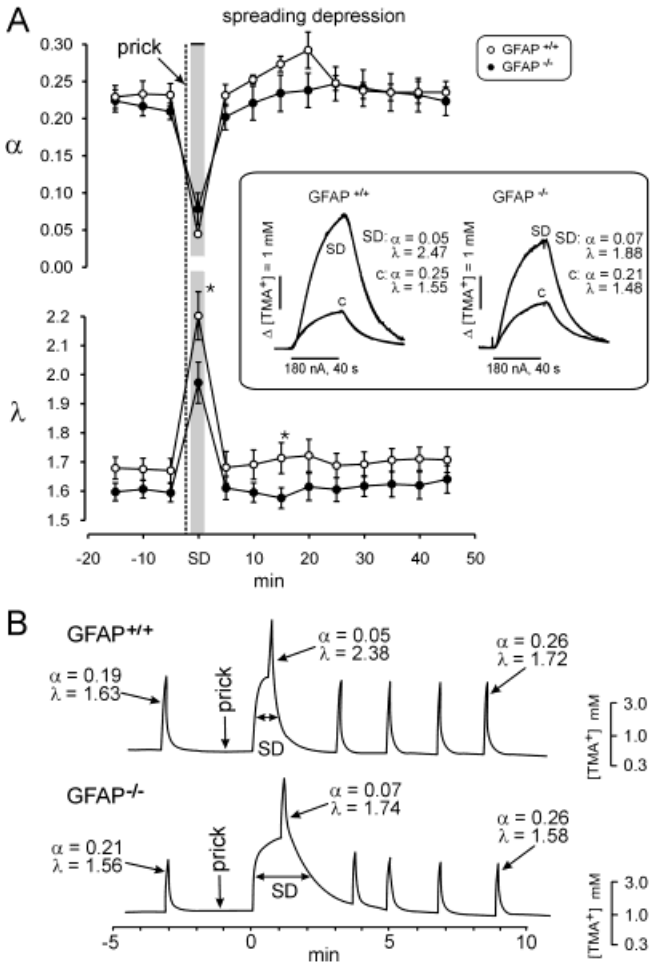

Fig. 7. The time course of changes in ECS volume fraction (α) and tortuosity (λ) during and after spreading depression (**A**) in the somatosensory cortex of adult $GFAP^{+/+}$ and $GFAP^{-/-}$ mice and typical diffusion curves (A inset). A inset: Normalized diffusion curves obtained before (c = control) and during spreading depression (SD) are shown with corresponding values of α and λ (array spacing r = 138 μm, transport number n = 0.336). A: α and λ were recorded at 5-min intervals before, during, and after spreading depression. Statistically significant differences between the values obtained in $GFAP^{+/+}$ and $GFAP^{-/-}$ mice are marked with asterisks (unpaired *t*-test, $P < 0.05$). **B:** Changes in TMA^+ extracellular concentration before, during, and after spreading depression. A certain nonzero concentration of TMA^+ in the tissue was maintained by continuous application of a small bias current (20 nA). Spreading depression (evoked by needle prick) is accompanied by an increase in TMA^+ extracellular concentration due to cell swelling. Diffusion curves (iontophoretic current of 200 nA) are superimposed and their respective diffusion parameters shown. Note that the duration of spreading depression in $GFAP^{-/-}$ mice is prolonged.

small in relation to the resting K^+ conductance. Our experiments show that $[K^+]_e$ after a depolarizing prepulse is lower in the vicinity of $GFAP^{-/-}$ astrocytes than around $GFAP^{+/+}$ astrocytes, and thus reveal the regional differences in the ECS around these cells. After the offset of a depolarizing prepulse, at least two events are involved in the clearance of increased K^+ from the vicinity of the astrocyte membrane: diffusion of K^+ into the ECS and K^+ uptake into the cells. Astrocytes are characterized by small tail currents after the offset of depolarization, therefore we suggest that only a small amount of K^+ re-enters the astrocyte and most of the K^+ released by depolarization diffuses into the ECS and is probably taken up by other glial cells. Our suggestion is supported by previous observations that large tail currents after the offset of a depolarizing prepulse in oligodendocytes are caused by an influx of K^+ into the cell (Berger et al., 1991; Chvátal et al., 1999). Because the conductance of the membrane during a depolarizing prepulse in $GFAP^{-/-}$ and $GFAP^{+/+}$ astrocytes is comparable, it is possible to assume that the depolarizing prepulse causes an efflux of the same amount of K^+ from the cell. A smaller increase in $[K^+]_e$ around $GFAP^{-/-}$ astrocytes after a depolarizing prepulse could therefore be explained by faster diffusion of K^+ from the immediate vicinity of the astrocyte membranes, probably resulting from fewer diffusion barriers around $GFAP^{-/-}$ astrocytes. Our hypothesis of faster K^+ flow through the less compact

*TABLE 3. Values of α, λ, and k′ Before, During, and After Spreading Depression (SD) in the Cerebral Cortex of GFAP$^{+/+}$ and GFAP$^{-/-}$ Mice**

	Control	SD	20 min after SD	40 min after SD
GFAP$^{+/+}$				
α	0.23 ± 0.02	0.05 ± 0.01[a]	0.26 ± 0.01	0.25 ± 0.02
λ	1.67 ± 0.04	2.29 ± 0.10[a]	1.69 ± 0.04	1.70 ± 0.04
k′	10 ± 3	37 ± 5[a]	14 ± 8	9 ± 2
n	6	3	6	5
GFAP$^{-/-}$				
α	0.22 ± 0.01	0.08 ± 0.02[b]	0.23 ± 0.02	0.24 ± 0.03
λ	1.59 ± 0.03	1.97 ± 0.07[b,c]	1.61 ± 0.03	1.60 ± 0.04
k′	10 ± 4	28 ± 8[a]	13 ± 5	11 ± 5
n	7	7	7	6

*The values of the extracellular volume fraction α, tortuosity λ, and nonspecific uptake k′ ($\times 10^{-3}$ s^{-1}) before, at the time of maximal change evoked by spreading depression, and 20 and 40 min after SD in GFAP$^{+/+}$ and GFAP$^{-/-}$ mice. Statistical significance was evaluated as the difference between GFAP$^{+/+}$ and GFAP$^{-/-}$ mice (c, unpaired, two-tailed *t*-test) and as the difference between control values before SD and the values during and after SD (a and b, paired, two-tailed *t*-test).
[a] $P < 0.05$.
[b] $P < 0.01$.
[c] $P < 0.05$.

ECS in the vicinity of GFAP$^{-/-}$ astrocytes is supported by the fact that most GFAP$^{-/-}$ astrocytes exhibited a reduced number and width of processes in comparison to GFAP$^{+/+}$ astrocytes. Therefore, the smaller cross-sectional diameter of GFAP-deficient astrocyte processes, also shown by McCall et al. (1996), and the reduced number of processes observed in our experiments may result in reduced K^+ accumulation after a depolarizing prepulse. It is also reasonable to assume that not only astrocytic processes but also the proteins of the extracellular matrix or adhesion molecules produced by astrocytes (Viggiano et al., 2000) might affect the ECS in the close vicinity of the astrocytic membrane and thus the flow of K^+ from the cell.

In contrast to the smaller K^+ accumulation in the vicinity of GFAP$^{-/-}$ than GFAP$^{+/+}$ astrocytes, we found no differences in the ECS diffusion parameters of spinal cord gray matter between GFAP$^{+/+}$ and GFAP$^{-/-}$ mice under physiological conditions. This may result from the fact that changes in $[K^+]_e$ are measured in the close vicinity of the astrocyte membrane, while diffusion parameters are measured over a volume of the order of 10^{-3} mm^3, which includes glial cells, neurons, cell processes, and macromolecules of the extracellular matrix forming diffusion barriers. In the cortex, λ was significantly lower in GFAP$^{-/-}$ mice, α and k′ were similar to controls.

Effect of Cell Swelling on Membrane Properties and ECS Diffusion Parameters

During cell swelling, evoked either by 50 mM K^+ or by hypo-osmotic stress, the difference between K^+ accumulation in the vicinity of GFAP$^{-/-}$ and GFAP$^{+/+}$ astrocytes evoked by a depolarizing prepulse and ECS diffusion parameter changes became more pronounced. In GFAP$^{+/+}$ astrocytes, $\Delta[K^+]_e$ calculated during the application of 50 mM K^+ or hypotonic solution was similar to that observed in astrocytes in the dorsal horn of rat spinal cord slices (Chvátal et. al. 1999); however $\Delta [K^+]_e$ observed in the vicinity of GFAP$^{-/-}$ astrocytes was much smaller. Since the amplitude of the depolarizing prepulse and the intracellular concentration of K^+ remained unchanged, one possible explanation for this finding could be restricted swelling of GFAP$^{-/-}$ astrocytes and therefore a smaller decrease in the ECS volume available for K^+ accumulation in the vicinity of the cell.

Swelling of astrocytes in isotonic ACF containing high K^+ or in hypotonic ACF has been described for many tissue cultures (Moller et al., 1974; Walz and Mukerji, 1988; Petito et al., 1991; Walz, 1992; Kimelberg et al., 1995). In our experiments, the application of hypo-osmotic solution evoked a hyperpolarization of astrocytes in contrast to the depolarization observed under the same conditions in cell culture experiments (Kimelberg and O'Connor, 1988; Kimelberg and Kettenmann, 1990; Vargová et al., 2001). In addition to increased membrane conductance during the application of hypo-osmotic solution, cell volume regulation involves a number of distinct ionic channels, transporters, and carriers, which can be different in astrocytes in situ and in vitro, and therefore the observed difference in their response to hypo-osmotic solution may arise from the different membrane properties of glial cells in culture and in acute brain slices. In experiments performed in vivo or in situ in relatively thick slices (400 μm in our experiments), it was shown that during cell swelling water moves from the extra- to the intracellular compartments and produces a decrease in ECS volume and an increase in tortuosity (Syková, 1997; Nicholson and Syková, 1998; Syková et al. 1999). Smaller ECS volume changes around GFAP$^{-/-}$ astrocytes during cell swelling, as calculated from V_{rev} of I_{tail}, are therefore in agreement with the changes in the ECS diffusion parameters, in which a larger decrease in α was observed in GFAP$^{+/+}$ than in GFAP$^{-/-}$ slices. These data are also compatible with previously reported findings showing 25%–46% lower release of taurine following hypotonic stress in primary cultures of reactive astrocytes devoid of IFs (GFAP$^{-/-}$ vimentin$^{-/-}$) (Ding et al., 1998).

Cortical spreading depression evoked changes in ECS diffusion parameters similar to those observed after K^+ application in vitro. This is not surprising, since the elevation of $[K^+]_e$ to 60 mM is a hallmark of this phenomenon. Similarly, the changes in GFAP$^{-/-}$ mice tended to be less pronounced than in GFAP$^{+/+}$ mice. The most interesting finding was the prolonged duration of the phenomenon. After superfusion of the slice with 50 mM K^+ and after SD, λ always returned to its control values in both GFAP$^{+/+}$ and GFAP$^{-/-}$ mice, while after application of a hypotonic solution λ remained increased in GFAP$^{-/-}$ slices. This might be explained by two different mechanisms of cell swelling, evoked by 50 mM K^+ or hypotonic solution, which may reflect differences in the ECS, including astrocytes

with their processes, neurons, proteins of the extracellular matrix, and adhesion molecules (Syková and Chvátal, 2000).

In $GFAP^{+/+}$ and $GFAP^{-/-}$ mice, the application of 50 mM K^+ results in a greater decrease in ECS volume and in much greater changes in ECS tortuosity than the application of a hypotonic solution. Syková et al. (1999) showed that the large increase in tortuosity found during cell swelling evoked by high K^+ is related to astrogliosis. It has also been reported that exposure to high K^+ results in increased immunoreactivity for GFAP (Canady et al., 1990; Del Bigio et al., 1994; Del Cerro et al., 1996). Furthermore, hypotonic solution results in hyperpolarization of glial cells to approximately −80 mV, while high K^+ results in depolarization of glial cells to −18 mV (Figs. 4 and 5). Such a depolarization may result in the activation of intracellular pathways and/or the release of neuroactive substances, e.g., ions and neurotransmitters, which may affect the composition of the ECS and may also explain the greater changes in ECS volume and tortuosity observed during the application of high K^+ in comparison to hypotonic stress.

Using $GFAP^{-/-}$ mice as a model system, we have shown that GFAP and intermediate filaments affect the ability of astrocytes to control their volume during swelling and therefore may play an important role during repetitive neuronal activity and pathological states such as spreading depression, seizures, and anoxia/ischemia.

REFERENCES

Ballanyi K, Grafe P, ten Bruggencate G. 1987. Ion activities and potassium uptake mechanisms of glial cells in guinea-pig olfactory cortex slices. J Physiol (Lond) 3820:1590–1740.

Berger T, Schnitzer J, Kettenmann H. 1991. Developmental changes in the membrane current pattern, K^+ buffer capacity and morphology of glial cells in the corpus callosum slice. J Neurosci 11:3008–3024.

Bignami A, Eng LF, Dahl D, Uyeda CT. 1972. Localisation of the glial fibrillary acidic protein in astrocytes by immunofluorescence. Brain Res 43:429–435.

Bignami A, Dahl D. 1977. Specifity of the glial fibrillary acidic protein for astroglia. J Histochem Cytochem 25:466–469.

Bourke RS, Kimelberg HK, Nelson LR, Barron KD, Auen EL, Popp AJ, Waldman JB. 1980. Biology of glial swelling in experimental brain edema. Adv Neurol 28:99–109.

Bureš J, Burešová O, Křivánek J. 1974. The mechanism and application of Leao's spreading depression of electrocephalographic activity. New York: Academic Press.

Canady KS, Ali-Osman F, Rubel EW. 1990. Extracellular potassium influences DNA and protein synthesis and glial fibrillary acidic protein expression in cultured glial cells. Glia 3:368–374.

Chen WJ, Liem RK. 1994. Reexpression of glial fibrillary acidic protein rescues the ability of astrocytoma cells to form processes in response to neurons. J Cell Biol 127:813–823.

Chiang J, Kowanda M, Arnes, Wright RL, Majno G. 1968. Cerebral ischemia. III. vascular changes. Am J Pathol 52:455–462.

Chvátal A, Pastor A, Mauch M, Syková E, Kettenmann H. 1995. Distinct populations of identified glial cells in the developing rat spinal cord: ion channel properties and cell morphology. Eur J Neurosci 7:129–142.

Chvátal A, Berger T, Vořišek I, Orkand RK, Kettenmann H, Syková E. 1997. Changes in glial K^+ currents with decreased extracellular volume in developing rat white matter. J Neurosci Res 49:98–106.

Chvátal A, Anděrová M, Žiak D, Syková E. 1999. Glial depolarization evokes a larger potassium accumulation around oligodendrocytes than around astrocytes in gray matter of rat spinal cord slices. J Neurosci Res 56:493–505.

Chvátal A, Syková E. 2000. Glial influence on neuronal signaling. Prog Brain Res 125:199–216.

Chvátal A, Anděrová M, Žiak D, Orkand RK, Syková E. 2001. Membrane currents and morphological properties of neurons and glial cells in the spinal cord and filum terminale of the frog. Neurosci Res 40:23–35.

Del Bigio MR, Omara F, Fedoroff S. 1994. Astrocyte proliferation in culture following exposure to potassium ion. Neuroreport 5:639–641.

Del Cerro S, Garcia-Estrada J, Garcia-Segura LM. 1996. Neurosteroids modulate the reaction of astroglia to high extracellular potassium levels. Glia 18:293–305.

Ding M, Eliasson C, Betsholtz C, Hamberger A, Pekny M. 1998. Altered taurine release following hypotonic stress in astrocytes from mice deficient for GFAP and vimentin. Mol Brain Res 62:77–81.

Edwards FA, Konnerth A, Sakmann B, Takahashi T. 1989. A thin slice preparation for patch clamp recordings from neurones of the mammalian central nervous system. Pflügers Arch 414:600–612.

Eliasson C, Sahlgren C, Berthold CH, Stakeberg J, Celis JE, Betsholtz C, Eriksson JE, Pekny M. 1999. Intermediate filaments protein partnership in astrocytes. J Biol Chem 274:23996–24006.

Eng LF, Vanderhaeghen JJ, Bignami A, Gerstl B. 1971. An acidic protein isolated from fibrous astrocytes. Brain Res 28:351–354.

Eng LF, Ghirnikar RS, Lee YL. 2000. Glial fibrillary acidic protein: GFAP—31 years (1969–2000). Neurochem Res 9–10:1439–1451.

Gomi H, Yokoyama T, Fujimoto K, Ikeda T, Katoh A, Itoh T, Itohara S. 1995. Mice devoid of the glial fibrillary acidic protein develop normally and are susceptible to scrapie prions. Neuron 14:29–41.

Hamill OP, Marty E, Neher E, Sakmann B, Sigworth FJ. 1981. Improved patchclamp techniques for high resolution current recording from cells and cell-free membrane patches. Pflügers Arch 391:85–100.

Kettenmann H, Sonnhof U, Schachner M. 1983. Exclusive potassium dependence of the membrane potential in cultured mouse oligodendrocytes. J Neurosci 3:500–505.

Kimelberg HK, O'Connor ER. 1988. Swelling-induced depolarization of astrocyte potentials. Glia 1:219–224.

Kimelberg HK, Kettenmann H. 1990. Swelling-induced changes in electrophysiological properties of cultured astrocytes and oligodendrocytes. I. effects on membrane potentials, input impedance and cell-cell coupling. Brain Res 529:255–261.

Kimelberg HK, Sankar P, O'Connor ER, Jalonen T, Goderie SK. 1992. Functional consequences of astrocyte swelling. Prog Brain Res 94: 57–68.

Kimelberg HK, Rutledge E, Goderie S, Charniga C. 1995. Astrocytic swelling due to hypotonic or high K^+ medium causes inhibition of glutamate and aspartate uptake and increases their release. J Cereb Blood Flow Metab 15:409–416.

Kuffler SW, Nicholls JG, Orkand RK. 1966. Physiological properties of glial cells in the central nervous system of amphibia. J Neurophysiol 29:768–787.

Leao AAP. 1944. Spreading depression of activity in the cerebral cortex. J Neurophysiol 7:359–390.

Lascola CD, Kraig RP. 1996. Whole-cell chloride-currents in rat astrocytes accompany changes in cell morphology. J Neurosci 16: 2532–2545.

Lascola CD, Nelson DJ, Kraig RP. 1998. Cytoskeletal actin gates a Cl^- channel in neocortical astrocytes. J Neurosci 18:1679–1692.

Liedtke W, Edelmann W, Bieri PL, Chiu FC, Cowan NJ, Kucherlapati R, Raine CS. 1996. GFAP is necessary for the integrity of CNS white matter architecture and long-term maintenance of myelination. Neuron 17:607–615.

Long DM. 1981. Traumatic brain edema. Clin Neurosurg 29:174–202.

Ludvin Sk, Kosek JC, Eng LF. 1976. The topographic distribution of S-100 and GFA proteins in the adult brain: an immunohistochemical study using horseradish peroxidase labeling antibodies. J Comp Neurol 165:197–208.

Mazel T, Richter F, Vargová L, Syková E. 2001. Changes in extracellular space volume and geometry induced by cortical spreading depression in immature and adult rats. Physiol Res (in press).

McCall MA, Gregg RG, Behringer RR, Brenner M, Delaney CL, Calbreath EJ, Zhang CL, Pearce RA, Chiu SY, Messing A. 1996. Targeted deletion in astrocyte intermediate filament (Gfap) alters neuronal physiology. Proc Natl Acad Sci USA 93:6361–6366.

Moller M, Mollgard K, Lund-Andersen H, Hertz L. 1974. Concordance between morphological and biochemical estimates of fluid spaces in rat brain cortex slices. Exp Brain Res 21:299–314.

Nawashiro H, Messing A, Azzam N, Brenner M. 1998. Mice lacking GFAP are hypersensitive to traumatic cerebrospinal injury. Neuroreport 9:1691–1696.
Nicholson C, Phillips JM. 1981. Ion diffusion modified by tortuosity and volume fraction in the extracellular microenvironment of the rat cerebellum. J Physiol (Lond) 321:225–257.
Nicholson C, Syková E. 1998. Extracellular space structure revealed by diffusion analysis. Trends Neurosci 21:207–215.
Orkand RK, Nicholls JG, Kuffler SW. 1966. The effect of nerve impulses on the membrane potential of glial cells in the central nervous system of amphibia. J Neurophysiol 29:788–806.
Pastor A, Chvátal A, Syková E, Kettenmann H. 1995. Glycine- and GABA-activated currents in identified glial cells of the developing rat spinal cord slice. Eur J Neurosci 7:1188–1198.
Pekny M, Levéen P, Pekna M, Eliasson C, Berthold C-H, Westermark B, Betsholtz C. 1995. Mice lacking glial fibrillary acidic protein display astrocytes devoid of intermediate filaments but develop and reproduce normally, EMBO J 14:1590–1598.
Pekny M, Eliasson C, Chien LG, Kindblom R, Liem A, Hamberger A, Betsholtz C. 1998a. GFAP-deficient astrocytes in vitro are capable of stellation when co-cultured with neurons and exhibite a reduced amount of intermediate filaments and an increased cell saturation density. Exp Cell Res 239:332–343.
Pekny M, Stanness KA, Eliasson C, Betsholtz C, Janigro D. 1998b. Impaired induction of blood-brain barrier properties in aortic endothelial cells by astrocytes from GFAP-deficient mice. Glia 22:390–400.
Pekny M, Johansson CB, Eliasson C, Stakeberg J, Wallén A, Perlmann T, Lendahl U, Betsholtz C, Berthold CH, Frisén J. 1999. Abnormal reaction to central nervous system injury in mice lacking glial fibrillary acidic protein and vimentin. J Cell Biol 145:503–514.
Petito CK, Juurlink BH, Hertz L. 1991. In vitro models differentiating between direct and indirect effects of ischemia on astrocytes. Exp Neurol 113:364–372.
Rutka JT, Smith SL. 1993. Transfection of human astrocytoma cells with glial fibrillary acidic protein complementary DNA: analysis of expression, proliferation, and tumorigenicity. Cancer Res 53:3624–3631.
Rutka JT, Hubbard SL, Fukuyama K, Matsuzava K, Dirks PB, Becker LE. 1994. Effects of antisense glial fibrillary acidic protein complementary DNA on the growth, invasion, and adhesion of human astrocytoma cells. Cancer Res 54:3267–3272.
Shibuki K, Gomi H, Chen L, Bao S, Kim JJ, Wakatsuki H, Fujisaki K, Fujimoto K, Katoh A, Ikeda T, Chen C, Thomson RF, Itohara S. 1996. Deficient cerebellar long-term depression, impaired eyeblink conditionig, and normal motor coordination in GFAP mutant mice. Neuron 16:587–599.
Svoboda J, Syková E. 1991. Extracellular space volume changes in the rat spinal cord produced by nerve stimulation and peripheral injury. Brain Res 560:216–224.
Syková E, Svoboda J, Polák J, Chvátal A. 1994. Extracellular volume fraction and diffusion characteristics during progressive ischemia and terminal anoxia in the spinal cord of the rat. J Cereb Blood Flow Metab 14:301–311.
Syková E. 1997. The extracellular space in the CNS: its regulation, volume and geometry in normal and pathological neuronal function. Neuroscientist 3:28–41.
Syková E, Vargová L, Prokopová Š, Šimonová Z. 1999. Glial swelling and astrogliosis produce diffusion barriers in the rat spinal cord. Glia 25:56–70.
Syková E, Chvátal A. 2000. Glial cells and volume transmission in the CNS. Neurochem Int 36:397–409.
Tatzelt J, Maeda N, Pekny M, Yang SL, Betsholtz C, Eliasson C, Camerino AP, DeArmond SJ, Prusiner SB. 1996. Scrapie in mice deficient for apoliprotein E or glial fibrillary acidic protein. Neurology 47:449–453.
Uyeda CT, Eng LF, Bignami A. 1972. Immunological study of the glial fibrillary acidic protein. Brain Res 37:81–89.
Vargová L, Chvátal A, Anděrová M, Kubinová Š, Žiak D, Syková E. 2001. Effect of osmotic stress on potassium accumulation around glial cells and extracellular space volume in rat spinal cord slices. J Neurosci Res (in press).
Viggiano D, Ibrahim M, Celio MR. 2000. Relationship between glia and the perineuronal nets of extracellular matrix in the rat cerebral cortex: importance for volume transmission in the brain. Prog Brain Res 125:193–198.
Voříšek I, Syková E. 1997. Ischemia-induced changes in the extracellular space diffusion parameters, K^+, and pH in the developing rat cortex and corpus callosum. J Cereb Blood Flow Metab 17:191–203.
Walz W, Mukerji, S 1988. KCl movements during potassium-induced cytotoxic swelling of cultured astrocytes. Exp Neurol 99:17–29.
Walz W. 1989. Role of glial cells in the regulation of the brain ion microenviroment. Prog Neurobiol 33:309–333.
Walz W. 1992. Mechanism of rapid K^+-induced swelling of mouse astrocytes. Neurosci Lett 135:243–246.
Weinstein DE, Shelanski ML, Liem RKH. 1991. Suppression by antisense mRNA demonstrates a requirement for the glial fibrillary acidic protein in the formation of stable astrocytic processes in response to neurons. J Cell Biol 112:1205–1213.